Intelligent Optimization Method for Core Flow Zoning of Long-Cycle Lead-Bismuth-Cooled Reactor

Qingyuan Yu[1], Shengqi Dai[1], Pengcheng Zhao[1,2]*, Yanan Zhao[1], Yingjie Xiao[1], Liangxing Peng[1] and Tao Yu[1]*

[1]School of Nuclear Science and Technology, University of South China, Hengyang, China, [2]Science and Technology on Reactor System Design Technology Laboratory, Nuclear Power Institute of China, Chengdu, China

Flow zoning is an important way to achieve core outlet temperature flattening. Appropriate zoning can improve safety and economy. This study combines an artificial intelligence optimization algorithm with a parallel multi-channel model to develop a model for calculating reactor core flow zoning based on the modern optimization theory, convergence analysis of a genetic algorithm, differential evolution algorithm, and quantum genetic algorithm is carried out for long-life reactor flow partitioning. Using the optimized algorithm, two flow rates are determined using power distribution at the beginning of the core life as the sample data and the maximum power of each fuel assembly during the entire life as the sample data. Comparative analysis of two different flow zoning schemes is implemented on a small long-life natural circulation lead-bismuth fast reactor, SPALLER-100. The findings of this study show that the quantum genetic algorithm has the best convergence for the long-life reactor among the three intelligent optimization algorithms, and it can quickly provide optimal results. In flow zoning scheme calculations based on the core power distribution at the beginning of reactor life, the maximum outlet temperature of the fuel assembly exceeds the thermal safety limit of the reactor, and in the flow zoning scheme calculations based on the average core power distribution during the whole reactor life, the maximum outlet temperature of the fuel assembly is 140 K lower than the maximum outlet temperature obtained in the previous scheme, remaining below the thermal safety limit. The optimal number of partitions for the SPALLER-100 reactor is determined to be 5, and increasing the number of zones only slightly improved the thermal safety performance of the reactor.

Keywords: lead-bismuth reactor, flow zoning, intelligent optimization algorithm, quantum genetic algorithm, safety performance

INTRODUCTION

From the perspective of thermal-hydraulic design, the core flow distribution of nuclear reactors is one of the most important issues. At the core outlet, the mixing of coolant temperatures causes temperature oscillation with a specific frequency and amplitude, resulting in thermal stress in the thermal measurement device and the central measurement column. Core flow zoning is an important means to realize core outlet temperature flattening. Flow distribution between different components is realized by opening specific component pins. High-power components have larger flows than low-power components, because of which, different components have similar outlet temperatures. The

non-uniform distribution of the outlet temperatures of the reactor core will greatly limit the operation life of the reactor. Reasonable zoning can improve the safety and economy of the reactor. Therefore, to improve the operation life of the long-life reactor and realize the rapid optimization of core outlet temperature flattening, it is urgent to develop a new core flow zoning method.

Flow zoning to ensure reactor safety and performance has been investigated by many researchers. Nagy et al. (2012) analyzed the influence of flow zoning on the life of a graphite-moderated of a molten salt reactor and examined the fuel proliferation efficiency. The fuel proliferation efficiency or the life of graphite was increased by separating the core into two radial regions with different amounts of graphite. Basualdo et al. (2020) coupled the sub-channel code SUBCHANFLOW with the reactor dynamics diffusion code PARCS. This coupling aimed to improve the physical model involved in the core analysis by enhancing the prediction accuracy. Moreover, it enabled the detailed prediction of local thermal-hydraulics parameters. Zhao et al. (Chen et al., 2014) developed a non-uniform heating parallel channel flow field calculation code for a small modular natural circulation lead- or lead alloy-cooled fast reactor (LFR) and compared it with the CFD method to verify the accuracy of the code, and then, based on the results of optimization analysis, they proposed a 10 MW natural circulation LFR core flow distribution optimization design. Liu et al. (Yizhe et al., 2012) developed the hydraulic characteristic calculation code DAEMON to calculate the flow distribution of the whole core under different working conditions, according to the design characteristics of the core and the primary circuit of the China Experimental Fast Reactor (CEFR). Zhou et al. (2018) developed and verified a code for the thermal-hydraulic design and optimization of a CFR600 fast reactor; the functions included in the code were fast reactor full-pile graphical modeling, fine sub-channel automatic division, thermal-hydraulic analysis considering heat transfer between components, and automatic flow zoning optimization. Li et al. (2019) divided the reactor core into external, middle, and internal fuel zones, calculated the minimum coolant flow required for each fuel assembly in each fuel zone, and then, divided the flow of the reactor core according to the different values of adjacent minimum coolant flows. Based on intelligent optimization algorithm, Wang et al. (2020) established the optimization model of flow partition design. Considering the maximum fuel temperature limit and the cladding temperature limit as boundary conditions, the total flow of the reactor core was minimized; the average temperature of the reactor core outlet was the highest, providing a novel method to address flow partition in large reactor cores. Zhang et al. (2017) used genetic algorithm (GA) and artificial neural network (ANN) (Cong et al., 2011) to predict CHF and succeeded to correlate the existing CHF data with better accuracy than the existing empirical correlations. Moreover, Chen et al. (2010) proposed mechanism-based correlations for LBB leakage by genetic algorithm. The presented correlations provide higher precision than the existing correlation.

With the increase of the number of fuel assemblies and partitions, resulting in poor convergence of the algorithm, longer time required
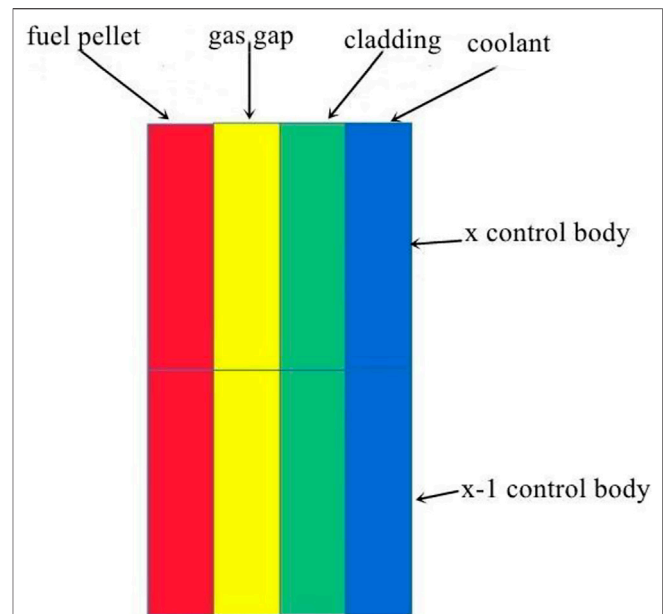

FIGURE 1 | Fuel rod heat conduction model.

for calculation, which cannot realize the rapid optimization design of core outlet temperature flattening. The power of each fuel assembly changes with changes in core life. In model establishment and calculation of results, the impact of different life periods on reactor power distribution should be considered. The designed flow zoning method should also ensure that the reactor is below the thermal safety limit during the entire life period. Based on the modern optimization theory, the study about artificial intelligence optimization algorithms with a parallel multi-channel model, and develops a reactor core flow zoning calculation model; the convergence of genetic algorithm, differential evolution algorithm, and quantum genetic algorithm for addressing the flow zoning problem of long-life reactors is analyzed, and the convergence optimal algorithm is obtained. According to the obtained optimal algorithm, for a small long-life natural circulation lead-bismuth fast reactor, SPALLER-100, considering two data samples, power distribution at the beginning of life and the maximum power of each fuel assembly in the whole life, two different flow zoning schemes are compared and analyzed, and the optimal flow zoning scheme is determined. It can be applied to other types of reactors to provide reference help for the design of the reactor, which will be strengthened in future study.

MATHEMATICAL PHYSICAL MODEL

Fuel Rod Heat Conduction Model

In this study, the fuel rod heat transfer model is used to describe the heat transfer process of a fuel rod in a reactor core, without considering the exchange of mass and momentum between channels. The heat conduction model is established using the rod bundle fuel rod, and its axial and radial control bodies are divided, as shown in **Figure 1**.

The axial heat conduction of fuel rods and the heat source inside the cladding are ignored, and the heat transfer between control bodies at a certain height in the core active zone is expressed as follows:

(1) Coolant controller:

$$Q(x) = Wc_p\left(t_{f,x} - t_{f,x-1}\right) \tag{1}$$

(2) External surface of the cladding control body:

$$t_{cs}(x) = t_f(x) + \frac{q_l(x)}{\pi d_{cs}h_x} \tag{2}$$

(3) External surface of the cladding control body:

$$t_{ci}(x) = t_{cs}(x) + \ln\left(d_{cs}/d_{ci}\right)\frac{q_l(x)}{2\pi k_{\text{clad}}} \tag{3}$$

(4) External surface of the fuel pellets control body:

$$t_u(x) = t_{ci}(x) + \ln\left(d_{ci}/d_u\right)\frac{q_l(x)}{2\pi k_{\text{gas}}} \tag{4}$$

(5) Fuel pellets control body central temperature:

$$t_o(x) = t_u(x) + \frac{q_l(x)}{4\pi k_u} \tag{5}$$

In the above equations, Q is the heat absorbed by the coolant (W), W is mass flow (kg/s), Cp is the average constant pressure specific heat capacity $(\text{J} \cdot \text{kg}^{-1} \cdot \text{K}^{-1})$, x is the axial control body symbol, $q_l(x)$ is the linear power density of the xth axial controller (W/m), h is the convective heat transfer coefficient $(\text{W} \cdot (\text{m}^{-2}\text{K}^{-1}))$, k_{cald} is the thermal conductivity of the cladding $(\text{W}/(\text{m} \cdot \text{K}))$, k_{gas} is the thermal conductivity of interstitial gas $(\text{W}/(\text{m} \cdot \text{K}))$, k_u is the thermal conductivity of the core $(\text{W}/(\text{m} \cdot \text{K}))$, d_{cs} is the largest outer diameter of fuel rods (m), d_{ci} is the inner diameter of the cladding (m), d_u is the core diameter (m), $t_f(x)$ is the temperature of the xth coolant control body (K), $t_{cs}(x)$ is the x cladding control body surface temperature (K); $t_{ci}(x)$ is the x cladding to control the body surface temperature (K), $t_u(x)$ is the x core control body surface temperature (K), $t_o(x)$ is the xth core control center temperature (K).

Parallel Multi-Channel Model

The parallel multi-channel model considers that the required heat pipe is isolated and closed. To facilitate calculation, it is assumed that there is no exchange momentum, energy, and mass of coolant with adjacent channels at any point in the core height. The parallel multi-channel model is most suitable for analyzing closed channels, but it can also be used for open channels to simplify calculation. Due to the existence of transverse mixing, the parallel multi-channel model is rough, and transverse mixing engineering heat pipe factors should be used to control increase in enthalpy. The parallel multi-channel model includes following steps.

(1) Enter data and determine the number of partitions.
(2) Identify the hottest pipe in each partition according to the partition scheme.
(3) Considering the reactor thermal-hydraulic pressure and core power distribution, determine the hottest tube of the cladding.
(4) Calculate the outlet temperature of the hottest pipe coolant, and obtain the hottest pipe flow in each zone.
(5) Calculate the total flow of the whole reactor, and obtain the average core outlet temperature (T_{out}) according to the relationship between the average core outlet temperature and the total reactor flow. The relationship between average core outlet temperature and total reactor flow is given as follows:

$$T_{out} = T_{in} + P\big/\left(C_pW\right) \tag{6}$$

where T_{in} is the core inlet temperature (K), P is the total core power (W).

Designing the Intelligent Optimization Algorithm for Life Cycle Traffic Zoning

The genetic algorithm (Zhang, 2017), differential evolution algorithm (Yang and Gu, 1997), and simulated annealing algorithm (Gai, 2017) are contemporary commonly used optimization algorithms. The novel quantum genetic algorithm (QGA) (Ying et al., 2018; Liu et al., 2020) provides new ideas for solving optimization problems. In this study, the genetic algorithm, differential evolution algorithm, and QGA are coupled with the parallel multi-channel model for determining the most suitable intelligent optimization algorithm to calculate the flow partition of a long-life miniaturized reactor, and then the convergence of each algorithm is analyzed. The calculation results of these three algorithms are compared, and the optimal algorithm to solve the core flow zoning problem is determined. The main steps of solving flow zoning are as follows.

(6) Import the initial data and design the initial partition scheme. The partition number (K), of this scheme starts from 1.
(7) For each component, the partition number k is randomly allocated between 1 and K.
(8) According to the partition results obtained in the second step, calculate the average core outlet temperature using the parallel multi-channel model.
(9) Obtain the optimal flow zoning scheme under the number of zones and its corresponding total core flow and average core outlet temperature. If the outlet temperature meets the requirements, output the zoning scheme to end the cycle. Otherwise, obtain a new zoning scheme using the intelligent optimization algorithm.
(10) Obtain another new partition scheme using the intelligent optimization algorithm.

In this study, three intelligent optimization algorithms will be used for calculation, namely, genetic algorithm, differential

evolution algorithm, and QGA. The main steps of the genetic and differential evolution algorithms are as follows.

Coding Design.

It is assumed that there are k possibilities in the flow area of each fuel assembly and s fuel assemblies in the whole core. To ensure that the algorithm can determine the optimal zoning scheme, the optimization domain should include all flow zoning schemes. The binary code is used to code the m_i of the fuel assembly flow zone, and the required binary bit number is $\log_2 K$ up integer, denoted as T. For example, when the number of zones is 4, the required binary bit number is 2, and the binary codes of flow areas 1–4 are 00, 01, 10, and 11, respectively.

Individual Fitness Design.

To achieve the optimization goal of minimizing the total core flow in the flow area, the fitness function is defined as:

$$Fit = \sum_{j=1}^{K} \left(n_j \cdot \min q_j \right) \quad (7)$$

where K is the number of zones, j is the number of the flow zone, and n_j is the number of fuel assemblies in the jth flow zone. $\min q_j$ is the minimum flow rate required by the maximum power component in the jth flow zone, which is determined by the fuel rod temperature limit, that is, the minimum flow not exceeding the temperature limit.

Evolution and Mutation.

This is the core step of the three algorithms, and it is also what differentiates them. The genetic algorithm and the differential evolution algorithm use the same evolutionary operation but different mutation operations. The genetic algorithm performs mutation processing according to the previously set mutation operation, while differential genetic algorithm uses mutation vector to realize population evolution:

$$v_{i,G+1} = x_{best,G} + \lambda g \left(x_{r1,G} - x_{r2,G} \right) \quad (8)$$

where λ is a random number from [0,1], and $x_{r1,G}$ and $x_{2r,G}$ are different chromosomes.

The QGA combines two special operation methods, namely, quantum computing and genetic algorithm, and thus, it has the advantages of two operation methods and is a probabilistic optimization algorithm. QGA is based on the state vector representation of quantum, and the probability amplitude of quantum bit is applied to chromosome coding, because of which, a chromosome can express the superposition of multiple states. The quantum logic gate is used to realize the chromosome update operation, thereby realizing the optimal solution of the target.

The main differences between QGA and genetic algorithm is the different coding methods and the population evolution modes. QGA replaces the chromosome coding operator of genetic algorithm with a quantum bit probability symbol. The standard QGA uses a quantum revolving gate to update the population rather than the evolution and crossover operation used in the standard genetic algorithm. The quantum revolving gate and its renewal process are given as follows:

TABLE 1 | Quantum rotation gate updating table.

x_i	b_i	$f(x_i) \geq f(b_i)$	$\Delta \theta i$	$s(\alpha_i, \beta_i)$			
				$\alpha_i \beta_i > 0$	$\alpha_i \beta_i < 0$	$\alpha_i = 0$	$\beta_i = 0$
0	0	False	0	—	—	—	—
0	0	True	0	—	—	—	—
0	1	False	δ	+1	-1	0	±1
0	1	True	δ	−1	+1	±1	0
1	0	False	δ	−1	+1	±1	0
1	0	True	δ	+1	-1	0	±1
1	1	False	0	—	—	—	—
1	1	True	0	—	—	—	—

"—"— "nil";δ—;$\Delta\theta_i$—;b_i—;x_i—;f—.

$$U(\theta_i) = \begin{bmatrix} \cos(\theta_i) & -\sin(\theta_i) \\ \sin(\theta_i) & \cos(\theta_i) \end{bmatrix} \quad (9)$$

$$\begin{bmatrix} \alpha'_i \\ \beta'_i \end{bmatrix} = U(\theta_i) \begin{bmatrix} \alpha_i \\ \beta_i \end{bmatrix} = \begin{bmatrix} \cos(\theta_i) & -\sin(\theta_i) \\ \sin(\theta_i) & \cos(\theta_i) \end{bmatrix} \begin{bmatrix} \alpha_i \\ \beta_i \end{bmatrix} \quad (10)$$

$$\theta_i = s(\alpha_i, \beta_i) \Delta \theta_i \quad (11)$$

where $(\alpha_i, \beta_i)^T$ and $(\alpha'_i, \beta'_i)^T$ are the probability amplitudes before and after the update of the ith qubit rotation gate of the chromosome, respectively; U is the quantum rotation gate; θ_i is the rotation angle, calculated from **Equation 11**, and $\Delta\theta_i$ is the magnitude of the rotation angle; $s(\alpha_i, \beta_i)$ is the direction of rotation. The values of δ and $s(\alpha_i, \beta_i)$ are given by 8 cases consisting of x_i, b_i, $f(x_i)$ and $f(b_i)$. The specific value-giving strategy is shown in **Table 1**. Typically, $0.01\pi \leq \delta \leq 0.05\pi$.

Interpret the iterative steps of the algorithm: When the maximum number of iterative steps designed by the algorithm is reached, the original partition number is updated, K = K + 1, and then, return to the first step to continue the calculation. If the maximum number of iteration steps designed by the algorithm is not reached, the new partition scheme generated by the intelligent optimization algorithm is returned to the second step to continue the calculation. The algorithm flow is shown in **Figure 2**.

Algorithm Test

To test the rationality and convergence of the three algorithms in flow zoning, CEFR was selected as the research object to test the adaptability of the three intelligent optimization algorithms. The half core power distribution of CEFR is shown in **Figure 3**. Under the premise of considering the design margin, the limiting conditions were set as follows: the maximum temperature of the cladding is ≤569°C, the temperature of the fuel center is ≤2,100°C, and the number of zones is 4. The three intelligent optimization algorithms were used to calculate the traffic partition separately. According to the partition results, the results obtained by the three intelligent optimization algorithms were consistent. The CEFR traffic is divided into four zones, which is the same as the actual partition results. Therefore, all three intelligent optimization algorithms were
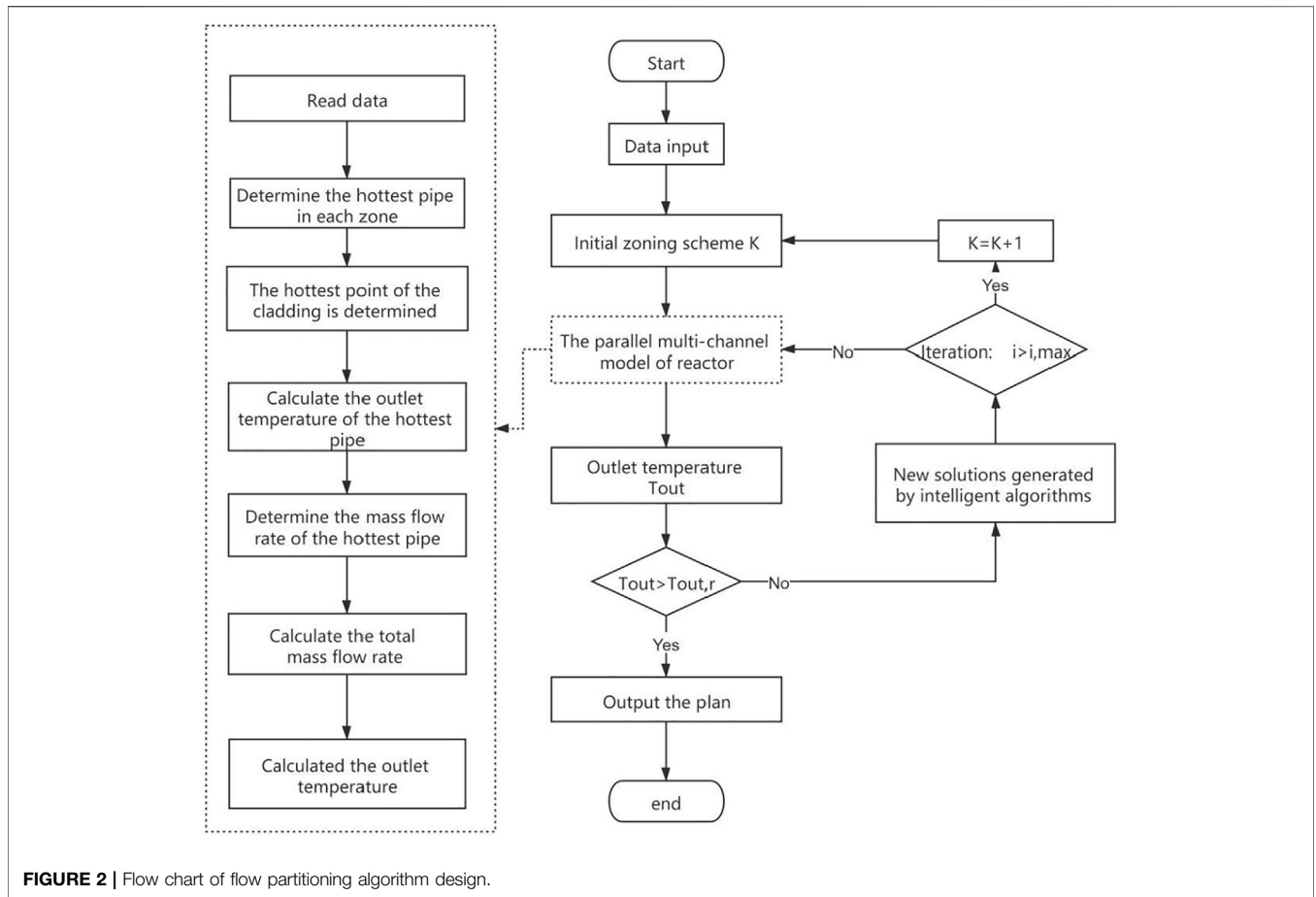
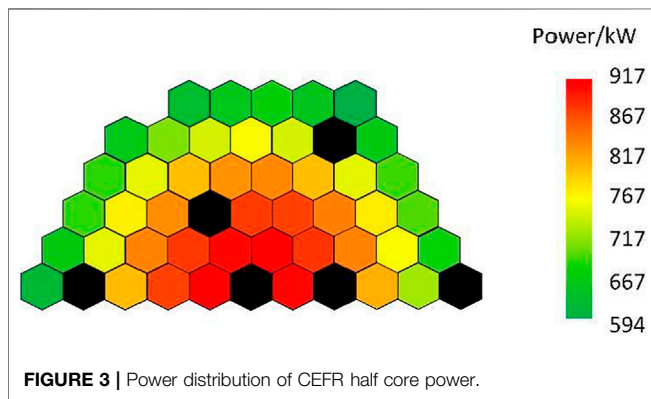**FIGURE 2 |** Flow chart of flow partitioning algorithm design.

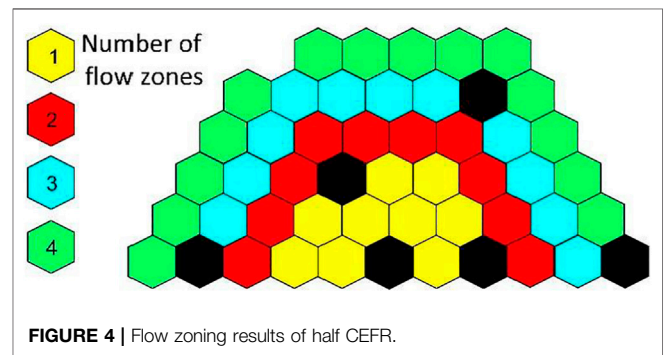**FIGURE 3 |** Power distribution of CEFR half core power.


FIGURE 4 | Flow zoning results of half CEFR.

feasible for traffic zoning. **Figure 4** shows the traffic partition schemes calculated using the three optimization algorithms.

Table 2 shows that the total iterative steps of QGA and genetic algorithm are set to 1,000 steps; the QGA tends to converge only after 101 iterations, and the calculation time is 13,368 s. The genetic algorithm converges after 316 iterations, and the calculation time is 15,757 s. Compared with the genetic algorithm, for the QGA, there was 15.16% reduction in time and 68.03% reduction in iteration steps. Therefore, the QGA has obvious advantages over the genetic algorithm in convergence

speed; however, the advantage in the speed of iterative calculation is not very obvious. Compared with the differential evolution method, the advantages of QGA are obviously reflected. The differential evolution algorithm has 1,298 convergence steps, and the total time consumption is 63,774 s. Comparatively, for QGA, there is 79.03% reduction in time and 92.21% reduction in iterative steps. Compared with the differential evolution algorithm, the QGA has obvious advantages in terms of total time consumption and convergence speed. Comparing these three algorithms, we know that the QGA has obvious advantages over the other two algorithms in terms of convergence steps and total time required for calculation, and

TABLE 2 | Algorithm convergence analysis results.

Algorithm Type	Total time(s)	Total Iteration Steps	Convergence Steps
Quantum genetic algorithm	13,368	1,000	101
Genetic algorithm	15,757	1,000	136
Differential evolution algorithm	63,774	1,500	1,298
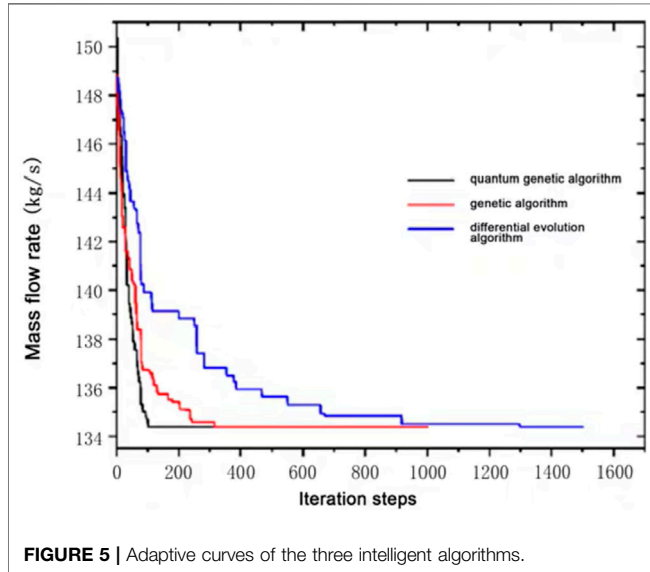
FIGURE 5 | Adaptive curves of the three intelligent algorithms.

it can be used as an intelligent optimization algorithm for the optimization of core flow zoning calculation of a long-life small reactor.

To compare the convergence between algorithms, adaptive curves of QGA intuitively, genetic algorithm, and differential evolution algorithm were extracted, as shown in **Figure 5**. QGA has obvious advantages in convergence compared with the other two algorithms. The final mass flows obtained by the three algorithms have relatively close values.

OPTIMIZATION OF SPALLER-100 FLOW ZONING DESIGN

SPALLER-100 Core Introduction

SPALLER-100 is a small long-life natural circulation lead- or lead-bismuth-based fast reactor that named SPALLER-100 designed at the University of South China. **Figure 6** shows the core section diagram of the SPALLER-100 reactor.

The thermal power of SPALLER-100 reactor core is 100 MW, the refueling cycle is 30 years, the operating temperature is 260–400°C, and the coolant temperature is 200°C under the condition of refueling shutdown. The height of the reactor core active zone is 1.5 m, and the equivalent diameter is 1.7 m. It comprises 48 fuel assemblies, 13 control rod components, 66 reflector components, and 126 shielding components. SPALLER-100 single fuel assembly has 61 fuel rods, and it uses PuN-ThN fuel. The effective density of fuel is 85% TD, and the cladding

material is HT-9. He is filled in the gap between the fuel pellet and the cladding. The diameter of the fuel pellet is 12 mm, and the thickness of the cladding is 0.6 mm. The inner diameter of the fuel rod is 12 mm, and the outer diameter is 13.5 mm. The in-pile loading of nuclear fuel is 5,475.88 kg, and the loading of fissile nuclides is 891.02 kg. The core activity is divided into internal and external zones. There are 12 fuel modules in the internal zone, with a Pu mass fraction of 20.5%, and 36 fuel modules in the external zone, with a Pu mass fraction of 30.8%. **Table 3** shows the limit conditions of thermal-hydraulic design for the SPALLER-100 reactor.

Design of Core Flow Zoning Scheme for SPALLER-100 Full Life Cycle

Based on the power distribution at the beginning of SPALLER-100 life, flow partition calculation was carried out using QGA. Flow rates for zones 1–4 were 79.14 kg/s, 72.26 kg/s, 65.05 kg/s and 57.85 kg/s, respectively. When the number of core zones was 4, the outlet temperature and mass flow rate of SPALLER-100 were 522.92°C and 3,143.38 kg/s, respectively. **Figure 7** shows the flow zoning scheme when the number of core zones is 4.

The containment temperature of the reactor was limited to 550°C. The closed channel model does not consider the transverse mixing between the components, thereby retaining the margin of 25°C. For the closed channel, the calculation results showed 24 boxes of fuel assembly with temperature >525°C in the whole life period; the outlet temperature of 12 boxes of fuel assembly was much higher than the limiting temperature. For the sub-channel, the calculation results showed 20 boxes of fuel assembly with temperature >550°C in the whole life period; the outlet temperature of 12 boxes of fuel assembly was much higher than the limiting temperature. It was concluded that the calculation of flow zoning based on the power distribution of a single time point can lead to serious security risks. Therefore, core flow zoning during the whole life period should be considered to ensure the safety of the core during operation.

The maximum power of each fuel assembly during the whole life of the reactor was considered as sample data, and whole life flow partition calculation was carried out for SPALLER-100. On this basis, the relationship between the minimum flow achieved by different partition numbers and the average outlet temperature of the active zone was analyzed, as illustrated in **Figure 8**.

Figure 8 shows that when the number of zones was 5, the average outlet temperature of the reactor core was close to saturation. Increasing the number of zones slightly improved the average outlet temperature of the reactor core, and so, it is reasonable to divide the reactor into five zones. The total core flow was 3,424.20 kg/s, and the average outlet temperature of the core
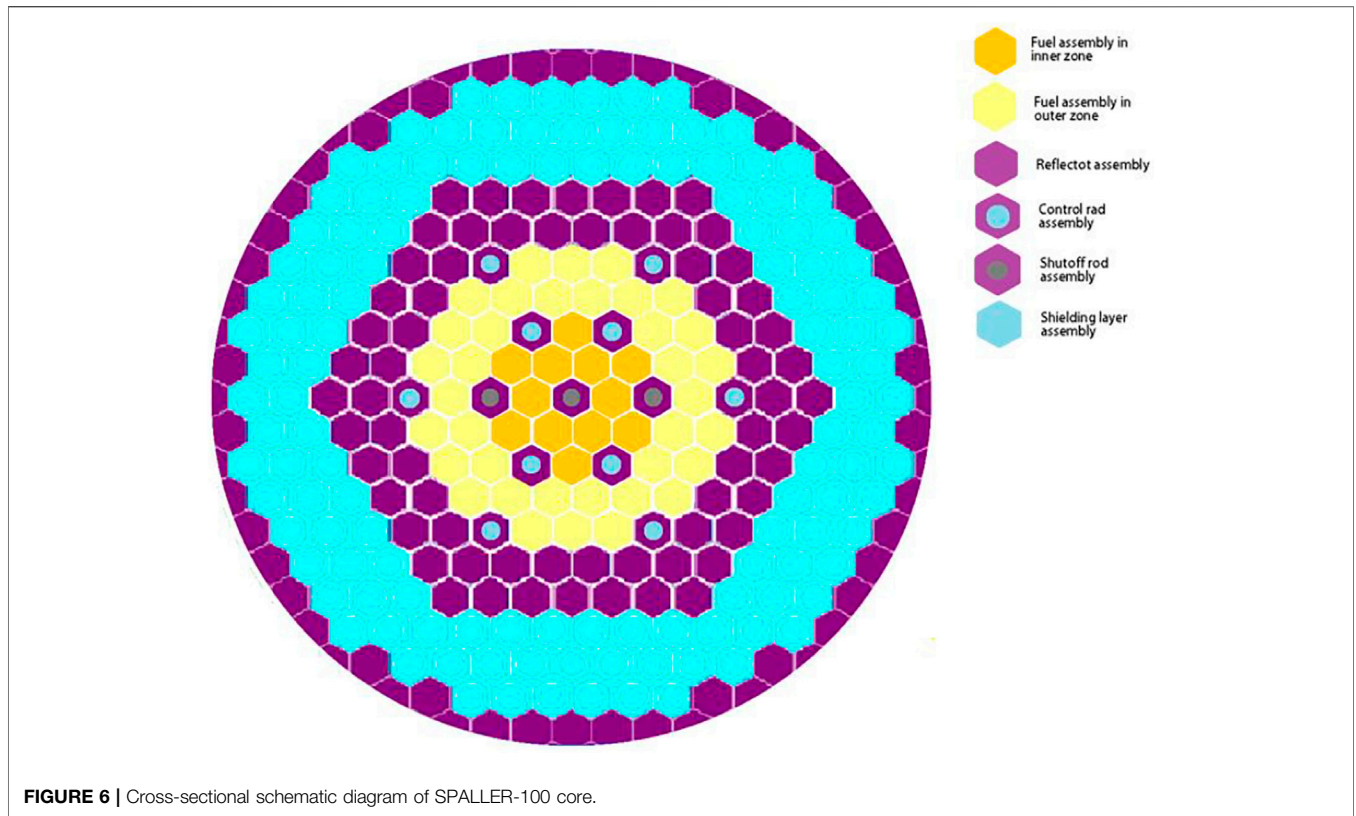
FIGURE 6 | Cross-sectional schematic diagram of SPALLER-100 core.

TABLE 3 | Thermal hydraulic design limits of SPALLER-100.

Project	Design Limit	
Maximum Temperature Limit of Fuel/°c	**2,300**	
Maximum temperature limit of cladding/°C	normal condition	550
	accident conditions	650
Maximum flow rate limit of coolant/(m/s)	2	
Minimum temperature of coolant/°C	200	

was 504.38°C. The partition results are shown in **Figure 9**. Flow rates of zones 1-5 are 82.36 kg/s, 79.14 kg/s, 72.29 kg/s, 60.05 kg/s and 58.00 kg/s, respectively.

Verification of SPALLER-100 Full Life Core Flow Zoning Scheme

To verify the accuracy of this procedure, the power of each component at 36 different times during the whole life of the reactor was extracted, and the maximum power of each component was selected as the sample data. The parallel multi-channel model designed in this study was used for calculations, and the calculated outlet temperature distribution is shown in **Figure 12**. The maximum power of each component was selected as the sample data. The fuel assemblies are shown in **Figure 10**, and the axial power distribution of the core is shown in **Figure 11**. These data were input into the card parameters, and the sub-channel code SUBCHANFLOW(Ferraro et al., 2020) was

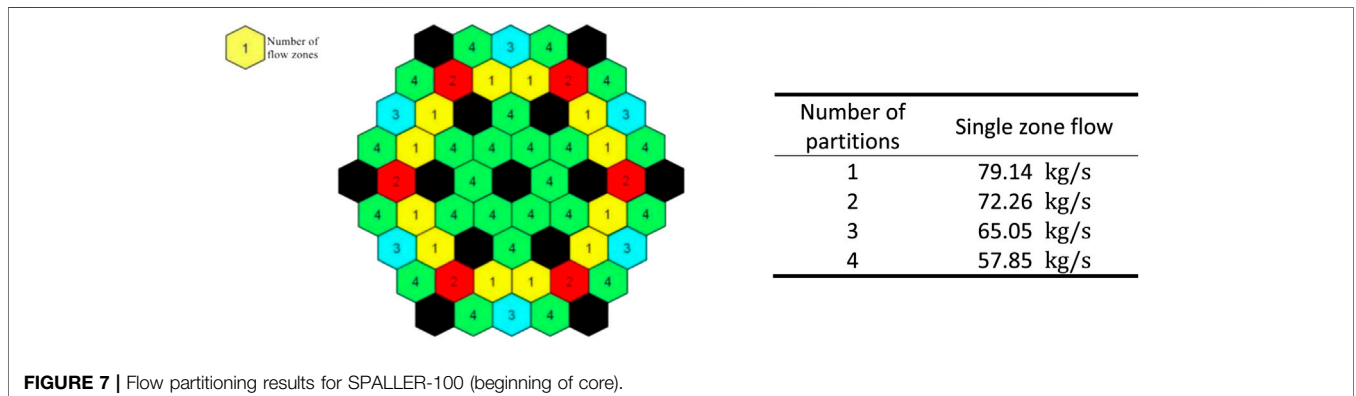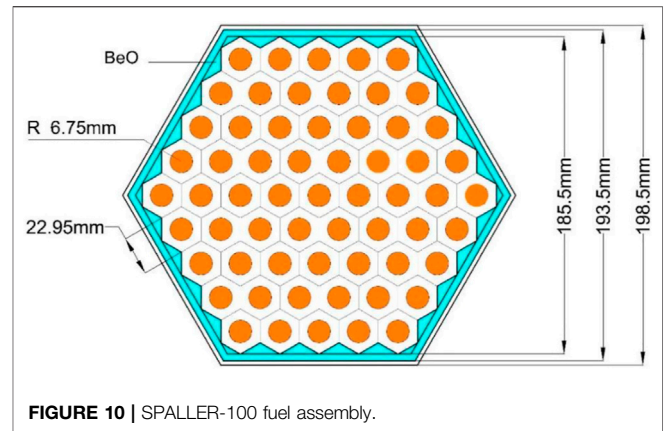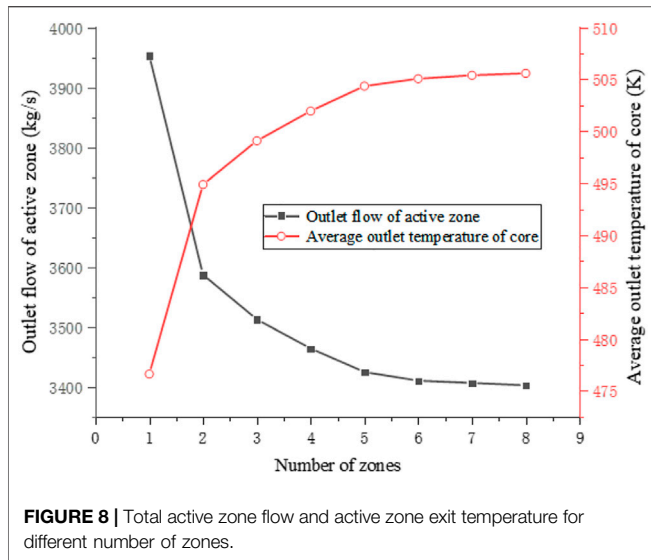| Number of partitions	Single zone flow
1	79.14 kg/s
2	72.26 kg/s
3	65.05 kg/s
4	57.85 kg/s

FIGURE 7 | Flow partitioning results for SPALLER-100 (beginning of core).

FIGURE 8 | Total active zone flow and active zone exit temperature for different number of zones.

FIGURE 10 | SPALLER-100 fuel assembly.

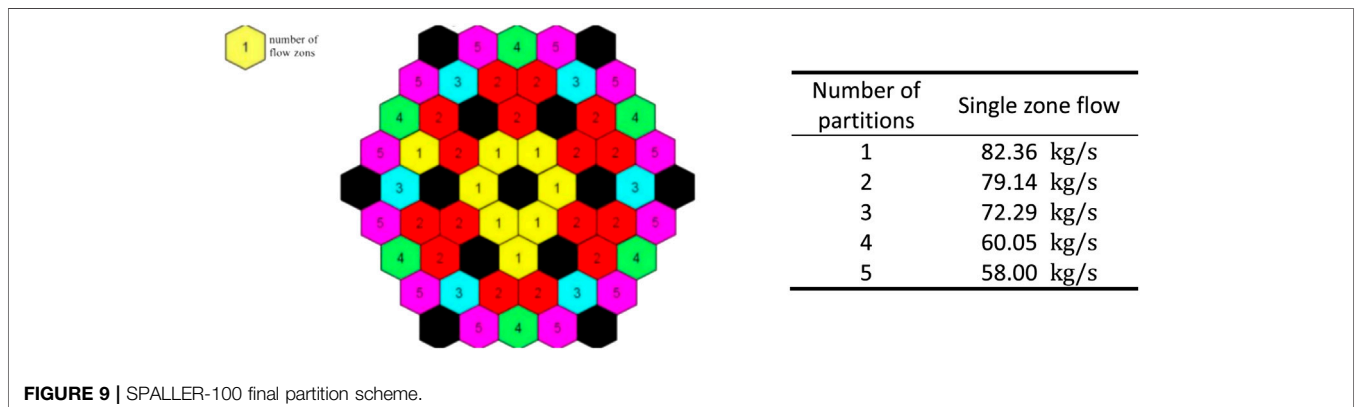used for calculation. The calculated outlet temperatures are presented in **Figure 13**.

Analyses shown in **Figure 12**, **Figure 13** show that under the same flow partition, the calculation results of the proposed model are in good agreement with the calculation results of the sub-channel code SUBCHANFLOW. The minimum relative error, the maximum relative error, and the average relative error were 0.5, 2.9, and 2.3%, respectively. Therefore, it can be considered that the calculation results of the proposed parallel multi-channel model design are sufficiently credible.
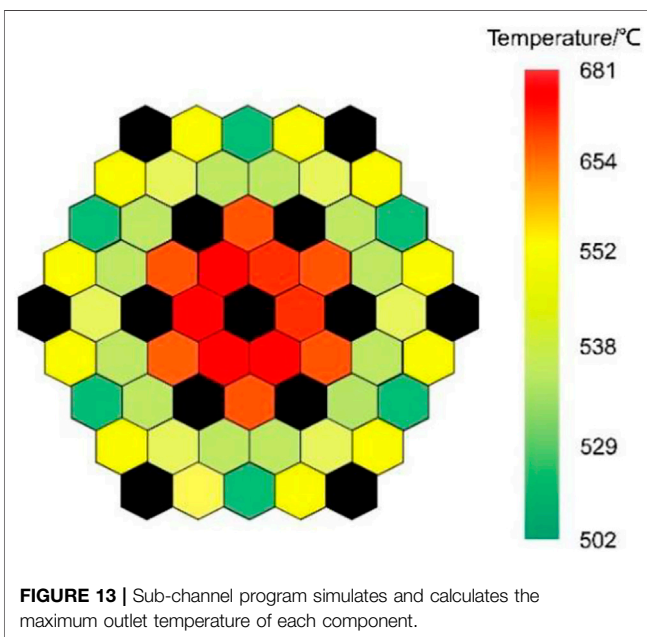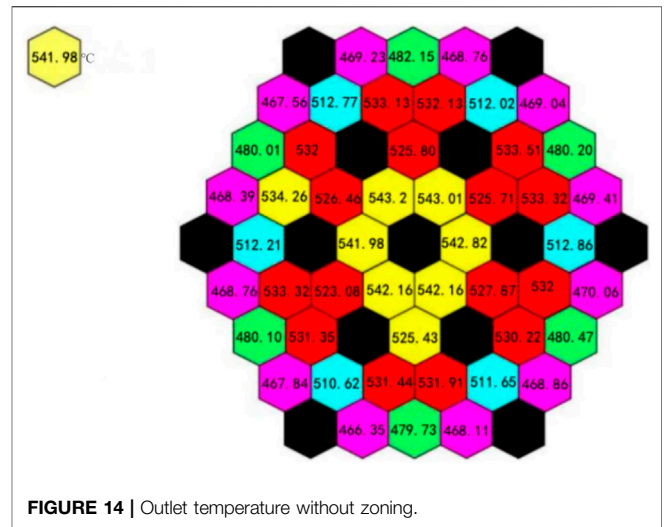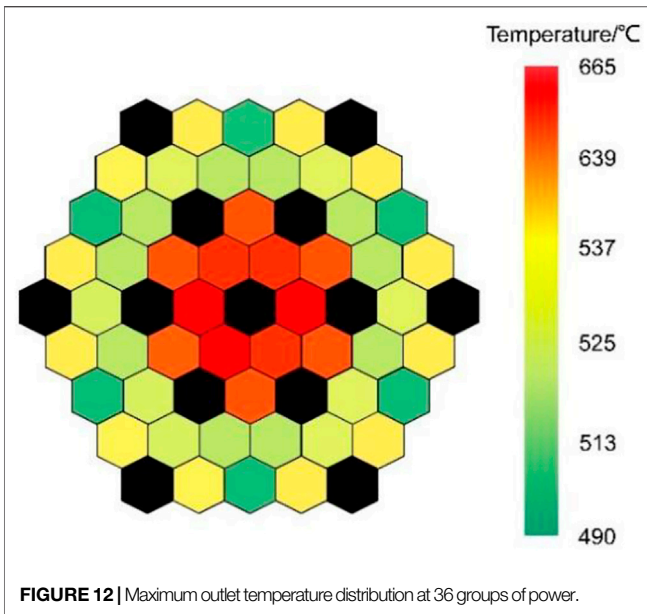
To verify the impact of flow zoning on the reactor core outlet temperature, the maximum power of each fuel assembly in the whole life was taken as sample data, and the coolant mass flow distribution of each fuel assembly in the core and the coolant outlet temperature of each fuel assembly without zoning were compared and analyzed. First, after partition treatment, the outlet temperature was calculated to obtain total coolant mass flow of each fuel assembly partition. Then, the coolant mass flow obtained above was averaged for each fuel assembly to obtain the outlet temperature without zoning. The SUBCHANFLOW program was used to calculate

FIGURE 11 | Axial power distribution of SPALLER-100.
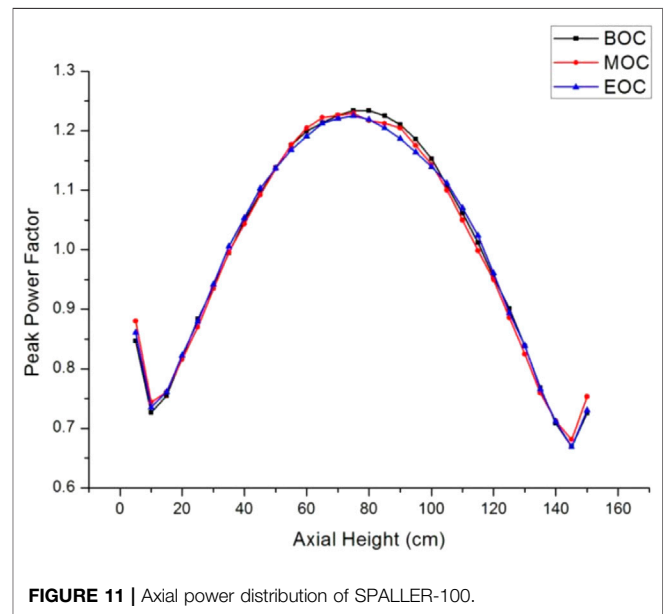
the results. According to the calculation results, the following conclusions were obtained.

When the core coolant was treated in zones, and the number of flow zones was 5, the average outlet temperature of the core coolant was 508.50°C; the difference between the maximum and

FIGURE 9 | SPALLER-100 final partition scheme.

Number of partitions	Single zone flow
1	82.36 kg/s
2	79.14 kg/s
3	72.29 kg/s
4	60.05 kg/s
5	58.00 kg/s

FIGURE 12 | Maximum outlet temperature distribution at 36 groups of power.

FIGURE 13 | Sub-channel program simulates and calculates the maximum outlet temperature of each component.

FIGURE 14 | Outlet temperature without zoning.

FIGURE 15 | Outlet temperature under zoning.

minimum temperatures was 22.44 °C. When the core coolant was not partitioned, the average coolant outlet temperature of the core was 507.82°C; the difference between the maximum and minimum temperatures was 76.85°C. When the total amount of coolant passing through remained unchanged, the average temperature change at the core outlet caused by the zoning and non-zoning treatments was slight, but the temperature fluctuation after zoning treatment is smaller; the difference between the maximum and minimum temperatures was small, and the outlet temperature was better flattened. Therefore, core flow treatment can flatten the core coolant outlet temperature. The detailed outlet temperatures are illustrated in **Figures 14**, **15**.

CONCLUSION

Reasonable core flow zoning of nuclear reactor can improve its safety and economy. Core flow zoning is also an essential means to flatten the core outlet temperature. Based on the modern optimization theory, artificial intelligence optimization algorithms were coupled with a parallel multi-channel model to construct a reactor core flow zoning calculation model. The convergence of different optimization algorithms was analyzed, and the optimal optimization algorithm was determined. This optimal optimization algorithm was used to carry out comparative analysis of two different flow zoning schemes using sample data of power distribution at the beginning of the life and the maximum power in the whole life of SPALLER-100. Following conclusions were obtained.

(1) Considering CEFR as the research object, for three intelligent optimization algorithms, namely, genetic

algorithm, differential evolution algorithm, and QGA, convergence analysis was carried out for reactor flow zoning. The results showed that QGA has the best convergence in long-life miniaturized reactor flow zoning, compared with the genetic algorithm. The total time consumption decreased by 15.16%. Compared with differential evolution algorithm, the total time consumption decreased by 79.03%.

(2) The flow zoning schemes designed based on the sample data of power distribution at the beginning of life and the maximum power of each fuel assembly in the whole life were compared and analyzed. The maximum outlet temperature of the fuel assembly based on the power distribution at the beginning of life exceeded the thermal safety limit of the reactor. Based on the power distribution of the whole reactor life, the maximum outlet temperature of the fuel assembly decreased by 140 K and was maintained below the thermal safety limit. The optimal number of zones of SPALLER-100 reactor at this time was 5. Increasing the number of zones led to challenges in flow distribution and did not significantly improve the thermal safety performance of the reactor.

(3) Flow zoning can bring a good flattening effect to the core outlet temperature. The SUBCHANFLOW program was used to analyze SPALLER-100. Taking the maximum power of the core in the whole life period as the calculation data, the following conclusions were obtained. When the core coolant was treated in zones and the number of flow zones was 5, the average outlet temperature of the core coolant was 508.50°C, and the difference between the maximum and minimum temperatures is 22.44°C. When the core coolant was not partitioned, the average coolant outlet temperature of the core was 507.82°C, and the difference between the maximum and minimum

temperatures was 76.85°C. When the total amount of coolant passing through remained unchanged, the average temperature change at the core outlet caused by zoning and non-zoning treatments was only slight; however, the temperature fluctuation after zoning treatment was smaller; the difference between the maximum and minimum temperatures was smaller, and the outlet temperature was better flattened. Therefore, core flow treatment can flatten core coolant outlet temperature.

DATA AVAILABILITY STATEMENT

The original contributions presented in the study are included in the article/Supplementary Material, further inquiries can be directed to the corresponding author.

AUTHOR CONTRIBUTIONS

QY: Data curation, Writing–original draft. SD: Conceptualization, Methodology, Software. PZ: Supervision. YZ: Visualization, Investigation. YX: Software, Validation. LP: Writing–review; editing. TY: Writing–review; editing.

REFERENCES

Basualdo, J. R., Sánchez-Espinoza, V., Stieglitz, R., and Macián-Juan, R. (2020). Integration of the Subchannel thermal-hydraulic Code SubChanFlow into the Reactor Dynamics Code PARCS: Development and Testing Based on a Computational Benchmark. *Prog. Nucl. Energ.* 119, 103138. doi:10.1016/j.pnucene.2019.103138

Chen, R. H., Su, G. H., Qiu, S. Z., and Fukuda, K. (2010). Prediction of CHF in Concentric-Tube Open Thermosiphon Using Artificial Neural Network and Genetic Algorithm. *Heat Mass. Transfer* 46 (3), 345–353. doi:10.1007/s00231-010-0575-9

Chen, Z., Zhao, P., Zhou, G., and Chen, H. (2014). Study of Core Flow Distribution for Small Modular Natural Circulation lead or lead-alloy Cooled Fast Reactors. *Ann. Nucl. Energ.* 72, 76–83. (in Chinese). doi:10.1016/j.anucene.2014.04.032

Cong, T., Chen, R., Su, G., Qiu, S., and Tian, W. (2011). Analysis of CHF in Saturated Forced Convective Boiling on a Heated Surface with Impinging Jets Using Artificial Neural Network and Genetic Algorithm. *Nucl. Eng. Des.* 241 (9), 3945–3951. doi:10.1016/j.nucengdes.2011.07.029

Ferraro, D., García, M., Valtavirta, V., Imke, U., Tuominen, R., Leppänen, J., et al. (2020). Serpent/SUBCHANFLOW Pin-By-Pin Coupled Transient Calculations for a PWR Minicore. *Ann. Nucl. Energ.* 137, 107090. doi:10.1016/j.anucene.2019.107090

Gai, J. (2017). *Improvement and Research of QuantumGenetic Algorithm[D]*. Jinzhou: Bohai University.

Li, S., Zhou, Z., and Feng, Y. (2019). *Coolant Flow Zoning Method in Fast Reactor core[P]*. BeiJing. CN109615110A-04-12(in Chinese).

Liu, Z., Zhao, P., and Zhang, B. (2020). Research on Core Concept Design of Ultra-long Life Small Natural Circulation Lead-based Fast Reactor[J]. *Nucl. Sci. Eng.* 54 (07), 1254–1265. (in Chinese). doi:10.7538/yzk.2019.youxian.0720

Nagy, K., Kloosterman, J. L., Lathouwers, D., and van der Hagen, T. H. J. J. (2012). The Effects of Core Zoning on the Graphite Lifespan and Breeding Gain of a Moderated Molten Salt Reactor. *Ann. Nucl. Energ.* 43, 19–25. doi:10.1016/j.anucene.2011.12.025

Wang, X., Wang, D., and Qi, S. (2020). Optimized Design Method for Core Flow Zoning of Sodium-Cooled Fast Reactor Based on Genetic Algorithm[J]. *Nucl. Sci. Eng.* 54 (09), 1660–1665. doi:10.7538/yzk.2020.youxian.0093

Yang, R., and Gu, J. (1997). An Efficient Simulated Annealing Algorithm for Global Optimization[J]. *Syst. Eng. —Theory Pract.* 17 (5), 30–33.

Ying, M., Wang, H., and L, H. (2018). Research on Self-Adaptive Quantum Genetic Algorithm. *Computer Eng. Appl.* 54 (20), 99–103.

Yizhe, L., Yijun, X., and Zhifeng, H. (2012). Calculation and Test of Core Flowrate Distribution of CEFR[J]. *Nucl. Sci. Eng.* 33 (S1), 100–103. (in Chinese).

Zhang, J., Chen, R. H., Wang, M. J., Tian, W. X., Su, G. H., and Qiu, S. Z. (2017). Prediction of LBB Leakage for Various Conditions by Genetic Neural Network and Genetic Algorithms. *Nucl. Eng. Des.* 325, 33–43. doi:10.1016/j.nucengdes.2017.09.027

Zhang, Q. (2017). *Research on Particle Swarm Optimization Algorithm and Differential Evolution algorithm[D]*. Jinan: Shandong University.

Zhou, Z., Yang, H., and Li, S. (2018). Preliminary Development of thermal-hydraulic Design Code for CFR600 Core [J]. *Nucl. Sci. Eng.* 52 (01), 56–63. (in Chinese). doi:10.7538/yzk.2020.youxian.0093